

## Elastic and inelastic scattering of $^{36}\text{Ar}$ on $^{208}\text{Pb}$ at 575 MeV beam energy

M. Bergmann, K.Th. Brinkmann, H. Freiesleben, and J. Kiesewetter

*Institut für Experimentalphysik I, Ruhr-Universität Bochum, D-4630 Bochum, Federal Republic of Germany*

D. Schüll and H. Sohlbach

*Gesellschaft für Schwerionenforschung, D-6100 Darmstadt 11, Federal Republic of Germany*

B. Kohlmeier and F. Pühlhofer

*Fachbereich Physik, Philipps-Universität Marburg, D-3550 Marburg, Federal Republic of Germany*

(Received 27 November 1989)

Elastic and inelastic scattering of 575 MeV  $^{36}\text{Ar}$  on  $^{208}\text{Pb}$  to low-lying states of both target and projectile nucleus were studied. The measured cross sections were analyzed with coupled-channels calculations. A very satisfying description of the data was obtained by using  $B(EL)$  values from the literature and proper optical potential parameters. The latter were used as basis to estimate the cross sections for the excitation of the isovector giant dipole and isoscalar giant quadrupole resonances.

### I. INTRODUCTION

Data of well resolved elastic and inelastic scattering of heavy ions only became available when high-resolution magnetic spectrometers became operational at heavy-ion accelerators. Both the energy region of low-lying states<sup>1-4</sup> and the high-energy nuclear continuum<sup>5-7</sup> were investigated. The analysis of the former data showed that coupling between channels must be taken into account in the determination of nucleus-nucleus optical potential parameters because of the sizable cross-section for inelastic excitations. The parameters were found to differ significantly from those obtained by poor-resolution experiments measured in the early days of heavy-ion physics.

The nuclear continuum below  $E^* \approx 30$  MeV is dominated by the excitation of giant resonances (GR) of various multipolarities as demonstrated by Bertrand *et al.*<sup>5</sup> in reactions of both 22A-MeV  $^{17}\text{O}$  and  $^{32}\text{S}$  with  $^{208}\text{Pb}$ , by Suomijärvi *et al.*<sup>7</sup> in reactions of 40A-MeV  $^{20}\text{Ne}$  with both  $^{90}\text{Zr}$  and  $^{208}\text{Pb}$  and by Rousset-Chomaz *et al.*<sup>2</sup> in reactions of 43A-MeV  $^{86}\text{Kr}$  on  $^{208}\text{Pb}$ . Other spectrometer data taken by Sohlbach *et al.*<sup>6</sup> at much lower beam energy ( $^{86}\text{Kr} + ^{208}\text{Pb}$  at  $E_{\text{lab}} = 18.2\text{A MeV}$ ) did not show prominent excitation of giant resonances. This finding is consistent with the observation of Ref. 8 that the cross-section for excitation of giant resonances in a certain nucleus increases with  $E/A$ .

Besides spectrometer data some time-of-flight data were also published. Chomaz *et al.*<sup>9</sup> reported the excitation of giant resonances in the  $^{36}\text{Ar} + ^{208}\text{Pb}$  system at low beam energy (11A MeV), which is very surpris-

ing in view of the above-mentioned findings. In particular the structures observed at high excitation energy, which were interpreted in terms of multiphonon excitations built from GR in the target nucleus,<sup>10</sup> caused considerable discussions.<sup>5,11-13</sup> were also found<sup>9</sup> in  $^{20}\text{Ne} + ^{208}\text{Pb}$  at 30A MeV and in various other nuclei<sup>14</sup> bombarded with 33A-MeV  $^{40}\text{Ar}$  applying the same experimental method.

It is the purpose of the present study to provide high-resolution spectrometer data for the  $^{36}\text{Ar} + ^{208}\text{Pb}$  system. The beam energy of 575 MeV ( $\approx 16\text{A MeV}$ ) is considerably higher than in the studies of Ref. 9. Excitation of low-lying collective states in both target and projectile nucleus are investigated; excitation of giant resonances, however, was not observed in the angular region studied. We will show in the present paper that a detailed analysis of elastic and inelastic scattering leads to reliable potential parameters on the basis of which cross sections for giant resonance excitation can be estimated.

### II. EXPERIMENTAL PROCEDURE AND RAW DATA

An  $^{36}\text{Ar}$  beam of 575 MeV from the UNILAC of GSI was used to irradiate self-supporting  $^{208}\text{Pb}$  targets of 270  $\mu\text{g}/\text{cm}^2$  area density isotopically enriched to 98.69%. The GSI magnetic spectrometer was used in combination with its focal plane detector to determine momentum spectra of outgoing projectile-like reaction products. The details of the experimental technique and the analyzing procedure were described in Refs. 6 and 15, respectively. An unambiguous identification of  $^{36}\text{Ar}$  and neighboring

ions in various charge states was achieved. In Fig. 1 we present the  $^{36}\text{Ar}$  momentum spectrum at  $\vartheta_{\text{lab}} = 20^\circ$  summed over the charge states  $q = 16^+, 17^+, 18^+$ , which contain more than 98% of the total charge state distribution. This spectrum covers excitation energies up to  $E^* \approx 50$  MeV. Besides the elastic line two inelastic peaks are clearly seen at  $E^* = (2.0 \pm 0.2)$  MeV and at  $E^* = (4.1 \pm 0.2)$  MeV. Within the experimental resolution of  $\Delta E = 1.2$  MeV ( $\Delta E/E = 2 \times 10^{-3}$ ) these peaks have to be identified with low-lying collective states in  $^{36}\text{Ar}$  and  $^{208}\text{Pb}$  known to be strongly excited in inelastic scattering of various probes, electrons as well as light and heavy ions (see Sec. III). These are  $2^+$  and  $3^-$  states, namely

$$^{36}\text{Ar}(2^+, 1.97 \text{ MeV}), \quad ^{208}\text{Pb}(3^-, 2.61 \text{ MeV})$$

on one hand and

$$^{208}\text{Pb}(2^+, 4.09 \text{ MeV}), \quad ^{36}\text{Ar}(3^-, 4.18 \text{ MeV})$$

on the other hand; they are compatible in energy with the observed peak positions. In the following these two experimental peaks are called “inelastic lines” although each of them comprises two states.

In the momentum spectrum of Fig. 1 these lines are followed by an inelastic continuum centered at  $E^* \approx 9$  MeV and a broad bump at  $E^* \approx 30$  MeV, the latter is due to the well known sequential particle emission after projectile pickup reactions.<sup>6</sup> There is no evidence for an excitation of giant resonances in  $^{208}\text{Pb}$  at  $E^* \approx 11$  MeV and  $E^* \approx 13.2$  MeV at this angle which is slightly forward of the grazing angle of  $\vartheta_{\text{lab}} = 20.2^\circ$ . We like to stress that the spectrometer’s hardware and software are so elaborate that the momentum spectra are essentially free of any artificial structures. Similar spectra were obtained at  $\vartheta_{\text{lab}} = 18^\circ$  and  $16^\circ$ , they were utilized to determine the cross section of the elastic and the inelastic lines. Spectra measured at more forward angles ( $14^\circ$ – $10^\circ$ ) allowed only the determination of the elastic scattering cross section, which rises extremely fast in comparison to the inelastic one, while at a more backward angle ( $\vartheta_{\text{lab}} = 22^\circ$ ) the

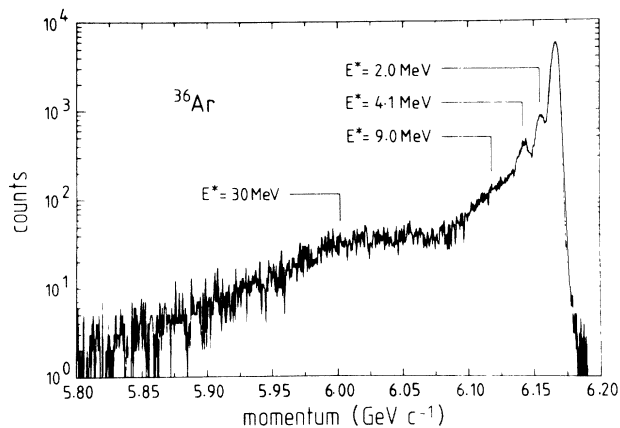


FIG. 1. Momentum spectrum of 575-MeV  $^{36}\text{Ar}$  scattered from  $^{208}\text{Pb}$  at  $\vartheta_{\text{lab}} = 20^\circ$ .

inelastic cross section became unmeasurably small in our experiment. The experimental cross sections for elastic and inelastic scattering will be compared to model calculations in the following section.

### III. MODEL CALCULATIONS FOR EXCITATION OF LOW-LYING STATES

Quantum-mechanical model calculations for elastic and inelastic scattering of heavy-ions can become very involved since a very large number of partial waves have to be considered. Therefore, the application of the generalized Fresnel model of Frahn and Gross<sup>16</sup> and the semi-quantal model of Frahn<sup>17</sup> for calculating  $E2$  excitations seem, at first, very attractive. Only the Coulomb and nuclear deformation lengths  $\delta_L^{(C)}$  and  $\delta_L^{(N)}$ , respectively, need to be known in the latter case. They are connected with the deformation parameters  $\beta_L^{(C)}$ ,  $\beta_L^{(N)}$  and the radii  $R_C$ ,  $R_N$  via the relation

$$\delta_L^{(C)} = \beta_L^{(C)} R_C, \quad \delta_L^{(N)} = \beta_L^{(N)} R_N,$$

where  $L$  refers to the multipolarity under consideration. The Coulomb deformation parameters  $\beta_L^{(C)}$  are connected with the  $B(EL)$  values for a target nucleus of charge  $Z_T e$  via

$$B(EL) = \left( \beta_L^{(C)} \frac{3}{4\pi} Z_T e R_C^L \right)^2$$

The size of the deformation length immediately shows that the weak-coupling condition implied in Frahn’s model<sup>17</sup> is not fulfilled in the present case. Hence a full quantum-mechanical coupled-channels calculation is needed.

Estimates of inelastic cross sections due to Coulomb excitation are commonly used to decide which transitions should be included in coupled-channels calculations. We used the Coulomb excitation code<sup>18</sup> COULEX to calculate angular distributions for the most prominent inelastic channels, which are listed in Table I together with the experimental  $B(EL)$  values taken from Finn<sup>19</sup> for  $^{36}\text{Ar}$  and from Ring and Speth<sup>20</sup> for  $^{208}\text{Pb}$ . The results

TABLE I. Reduced transition probabilities  $B(EL)$  for the excitation of various states in  $^{36}\text{Ar}$  and  $^{208}\text{Pb}$  taken from  $X(e, e')X$  scattering experiments (from Refs. 19 and 20).

$i$	Transitions $\rightarrow f$	$L$	$B(EL)$ $e^2 b^L$
$\text{Ar}(0^+)$	$\text{Ar}(2^+, 1.97 \text{ MeV})$	2	0.028
	$\text{Ar}(3^-, 4.18 \text{ MeV})$	3	0.0113
$\text{Pb}(0^+)$	$\text{Pb}(3^-, 2.61 \text{ MeV})$	3	0.6
	$\text{Pb}(2^+, 4.09 \text{ MeV})$	2	0.2965
	$\text{Pb}(4^+, 4.32 \text{ MeV})$	4	0.1287

TABLE II. Optical potential parameters for the system  $^{36}\text{Ar} + ^{208}\text{Pb}$  at 575 MeV, where  $V$  and  $W$  are the depth of real and imaginary Woods-Saxon potentials,  $R_r$ ,  $R_i$ , and  $R_C$  are the radii of the potentials, and  $a_r$  and  $a_i$  are the diffuseness of the potentials.

Set	$V$ (MeV)	$R_r$ (fm)	$a_r$ (fm)	$W$ (MeV)	$R_i$ (fm)	$a_i$ (fm)	$R_C$ (fm)
I	19.4	11.16	0.74	30.4	11.16	0.76	11.99
II	20.9	11.44	0.79	24.4	11.44	0.77	11.99
III	33.4	11.72	0.43	48.3	11.72	0.56	11.99

are depicted in Fig. 2 together with the experimental data of the elastic and the two “inelastic lines.” Only the most forward data points should be compared to the calculations since they are the ones least influenced by nuclear excitation. One concludes from this calculations that strong coupling to  $2^+$  states is likely to be present, that  $3^-$  excitations may be important via interference and that the excitation of  $4^+$  states can safely be neglected in the further investigation that includes the absorptive nuclear potential. This finding is the reason for attributing the two “inelastic lines” observed in the momentum spectrum of Fig. 1 to low-lying collective states of  $^{36}\text{Ar}$  and  $^{208}\text{Pb}$ .

Coupled-channels calculations were performed by using the code ECIS79 of Raynal.<sup>21</sup> At first, optical model parameters were determined by  $\chi^2$ -fitting of the differential cross section for elastic scattering and taking into account the  $E2$  couplings in both  $^{36}\text{Ar}$  and  $^{208}\text{Pb}$ . These excitations are calculated in the vibrational model assuming one-phonon excitations. Since there is no convincing evidence that the Coulomb and nuclear deformation lengths are different we used  $\delta_L^{(C)} = \delta_L^{(N)}$ ; their values were deduced from Table I. In order to obtain numerically stable results it was necessary to use an in-

tegration step size of 0.02 fm and a matching radius of 50 fm. Therefore partial waves up to  $\ell = 2700\hbar$  had to be taken into account. Three sets of optical model parameters were found to reproduce the experimental data almost equally well. They are listed in Table II. The calculated cross section for elastic and inelastic scattering is shown in Fig. 3 as a solid line (potential set II).

In a second step we also considered in the coupled-channels calculations  $3^-$  excitations of  $^{36}\text{Ar}$  and  $^{208}\text{Pb}$ . The optical potential parameter set II was used again. The inclusion of  $3^-$  excitations modifies only slightly the elastic and inelastic  $2^+$  cross sections as can be seen from the dashed lines in Fig. 3. The additive contributions are the results of constructive interferences due to  $3^-$  excitations. Their smallness fortunately justifies our procedure of not taking into account  $E3$  couplings dur-

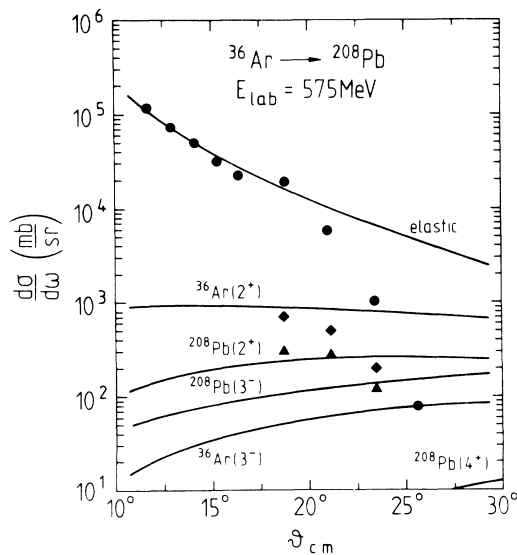


FIG. 2. Elastic and inelastic cross-section of various collectively excited states in  $^{36}\text{Ar}$  and  $^{208}\text{Pb}$  calculated with COULEX. Data points are included (circle: elastic line; diamond: “inelastic line 1”; triangle: “inelastic line 2”).

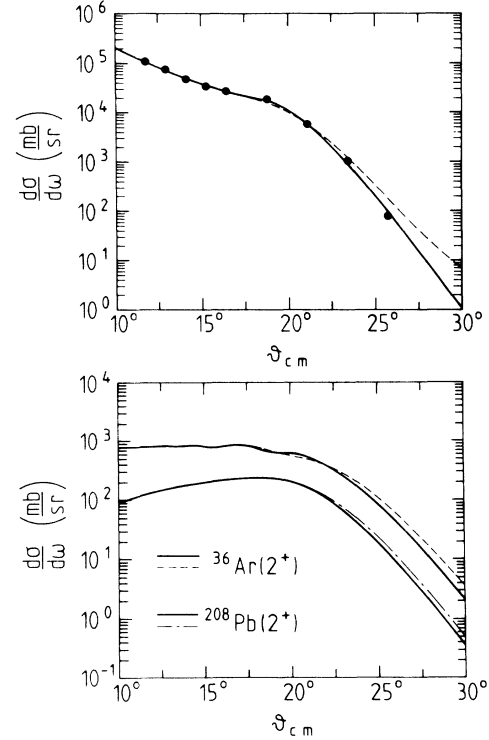


FIG. 3. Results of coupled-channels calculation. Top: (solid line) elastic differential cross section taking into account couplings to  $^{36}\text{Ar}(2^+)$  and  $^{208}\text{Pb}(2^+)$ . Bottom: (solid line) inelastic differential cross-section for  $^{36}\text{Ar}(2^+)$  and  $^{208}\text{Pb}(2^+)$ . The broken lines result if  $^{36}\text{Ar}(3^-)$  and  $^{208}\text{Pb}(3^-)$  excitations are additionally coupled in.

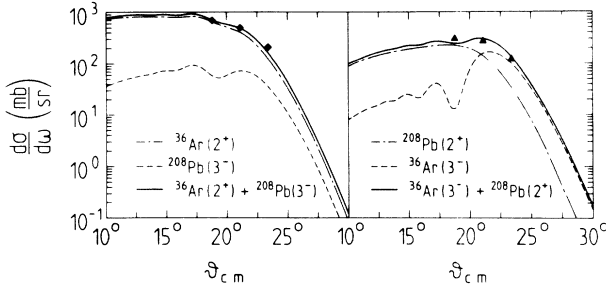


FIG. 4. Results of coupled-channels calculations for excitation of  $2^+$  and  $3^-$  states in both  $^{36}\text{Ar}$  and  $^{208}\text{Pb}$ . The left frame shows the sum of  $^{36}\text{Ar}(2^+)$  and  $^{208}\text{Pb}(3^-)$  differential cross sections together with the data for “line 1” (diamonds). The right frame shows the sum of  $^{208}\text{Pb}(2^+)$  and  $^{36}\text{Ar}(3^-)$  differential cross sections together with the data for “line 2” (triangles).

ing the  $\chi^2$ -fitting of optical model parameters. Including  $3^-$  excitations on top of  $2^+$  excitations would result in roughly three times longer computation times, which could not be justified in view of the smallness of the anticipated correction.

The calculated cross-sections for  $2^+$  and  $3^-$  excitations in  $^{36}\text{Ar}$   $^{208}\text{Pb}$  were added in order to render possible a comparison with the experimental data. The results are shown in Fig. 4. A surprisingly good agreement is found for both “inelastic lines.” The line at  $E^* \approx 2.0$  MeV is dominated by the  $2^+$  excitation of  $^{36}\text{Ar}$  (1.97 MeV) with the  $3^-$  excitation of  $^{208}\text{Pb}$  (2.61 MeV) being almost negligible. This is also reflected in the energetic position of this line. The line with centroid at  $E^* \approx 4.1$  MeV is clearly a superposition of the  $2^+$  state in  $^{208}\text{Pb}$  (4.09 MeV) and the  $3^-$  state in  $^{36}\text{Ar}$  (4.18 MeV), with the former (latter) one dominating at forward (backward) angles, the experimental data just covering the transition region.

We consider these results as encouraging in view of a quantitative understanding of experimental heavy-ion data measured with high resolution.

#### IV. MODEL CALCULATIONS FOR GIANT-RESONANCE EXCITATIONS

Giant resonances were studied frequently (see e.g., Ref. 22). In  $^{208}\text{Pb}$  the isovector giant dipole (GDR) at  $E_{IV}^* = 13.2$  MeV and isoscalar giant quadrupole resonance (GQR) at  $E_{IS}^* = 11$  MeV, respectively, are known to exhaust nearly 100% of the energy-weighted sum-rule (EWSR). Their resonance width is  $\Gamma_{GR} \approx 3$  MeV (cf. Ref. 22). They would be completely resolved from low-lying collective states in our experiment. However, in the investigated angular range there is no significant structure discernible in the measured  $^{36}\text{Ar}$  momentum or derived energy spectra that could be attributed to GR excitations. This result is quite surprising in view of the experimental results reported in Ref. 9. However, it is quantitatively corroborated by the following calcu-

lations.

First we performed Coulomb excitation calculations for states in  $^{208}\text{Pb}$  (cf. Fig. 5), including both the GDR and the GQR in lead. The strength function  $S(EL)$  of each GR was assumed to be represented by a  $\delta$  function located at the experimental energies  $E_L$ . Then the commonly used relation

$$S(EL) = E_L B(EL)$$

holds.  $S(EL)$  was calculated following Refs. 24 and 25:

$$S(E1) = \frac{9}{4\pi} \frac{\hbar^2}{2M} \frac{NZ}{A} e^2$$

and for  $L \geq 2$

$$S(EL) = \frac{L(2L+1)}{4\pi} \frac{\hbar^2}{2M} Z e^2 \langle R^{2L-2} \rangle,$$

where  $M$  is the nuclear mass unit in MeV and  $\langle R^p \rangle$  is the  $p$ th moment of a spherical charge distribution with radius  $R$ ,  $\langle R^p \rangle = 3/(p+3)R^p$ . Figure 5 shows the angular distribution of both giant resonances and that of the other states observed in  $^{208}\text{Pb}$ . This Coulomb excitation calculation shows that the GDR can safely be neglected in comparison to the GQR in the present situation, even in the case of a GR excitation with both, nuclear and Coulomb interaction.

We then performed coupled-channels calculations with the code ECIS-79, taking into account the excitations of  $^{36}\text{Ar}(2^+)$ , 1.97 MeV and  $^{208}\text{Pb}(2^+)$ , 4.09 MeV, which were found to be most strongly coupled to the elastic channel (see above), and that of the GQR in  $^{208}\text{Pb}$ . On basis of a 100% exhausted EWSR for  $E2$  excitations a deformation parameter of  $\beta_{GQR}^{(C)} = 0.0755$  is obtained in the vibrational model from the formula given above (cf. Ref. 22). Again the optical potential parameter set II from Sec. III and the equality of Coulomb and nuclear deformation,  $\delta^{(C)} = \delta^{(N)}$ , was assumed. Although it was argued that GR excitation proceeds dominantly by nuclear forces<sup>10</sup> we did not neglect Coulomb excita-

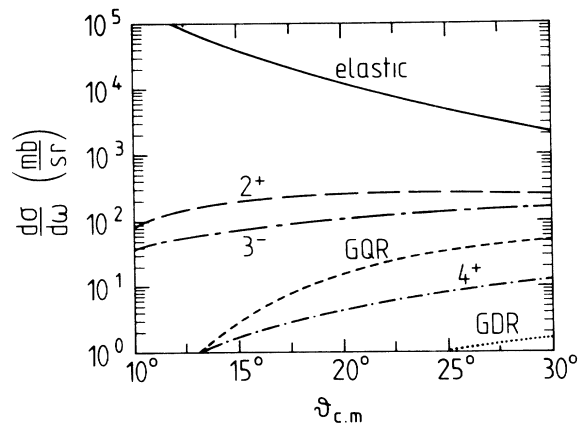


FIG. 5. Cross section for Coulomb excitation of various states in  $^{208}\text{Pb}$  (calculated with COULEX).

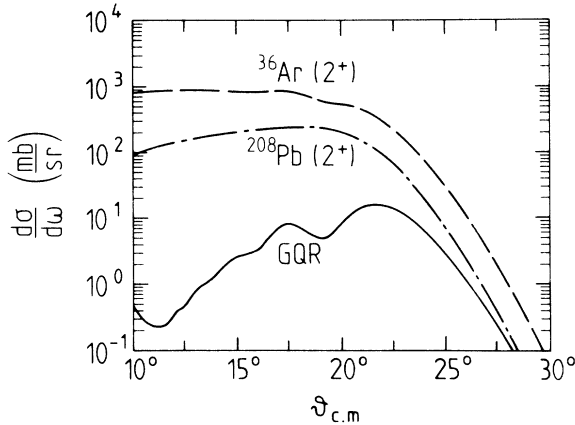


FIG. 6. Differential cross sections obtained from a coupled-channels calculation for  $^{36}\text{Ar}$  and  $^{208}\text{Pb}$ . Couplings of the indicated states to their respective ground states were taken into account.

tion in order to avoid a bias in the model calculations. Figure 6 depicts the results of the model calculation. At angles around the quarter point angle ( $\vartheta_{c.m.}^{1/4} = 22.2^\circ$ ) a differential cross section of  $\approx 15$  mb/sr is predicted for GQR excitation. This value fits nicely into the systematics presented by Sandorfi<sup>8</sup> of GQR excitation cross sections in  $^{208}\text{Pb}$  measured as a function of beam energy with various hadronic probes. We find Coulomb and nuclear excitation to be of equal importance in contrast to the above-mentioned conjecture.<sup>10</sup> The calculated GQR cross section is about a factor of 20 smaller than that for the added intensity of  $^{36}\text{Ar}$  ( $2^+$ , 1.97 MeV) and  $^{208}\text{Pb}$  ( $3^-$ , 2.61 MeV), represented by "line 1" in Fig. 1. Considering also the GQR width, which is about 3 times larger than that of "line 1," it is understood that the measured momentum spectrum does not exhibit pronounced GR structures. The cross section for GQR excitation decreases at more forward angles according to our calculations, and its observability is diminished in view of the rapidly growing elastic cross section.

Chomaz *et al.*<sup>9</sup> reported for the system  $^{36}\text{Ar} + ^{208}\text{Pb}$  at 11A MeV the excitation of giant resonances and high excitation energy structures. The latter were interpreted in

terms of target multiphonon excitations built from giant resonances.<sup>10</sup> A very comprehensive study of this process was published recently.<sup>23</sup> If the relative excitation probability calculated at the grazing angle for two phonon excitation,<sup>9</sup> which is about a factor of 40–50 smaller than that for one phonon excitation, holds also for our beam energy of 16A MeV we have no chance to observe the two phonon excitation. This quantitative argument can be turned around and may be used in disfavor of Refs. 9 and 10: The observed structures at high excitation energy<sup>9</sup> correspond to cross sections much larger than the model calculations<sup>10</sup> predict. Based on this observation and our data we conclude that the reported high excitation energy structures<sup>9</sup> are unlikely to be due to multiphonon target excitations. Their existence still needs to be proven.

## V. CONCLUDING REMARKS

We have shown in this paper that a consistent description of elastic and inelastic scattering to low-lying collective states in both projectile and target nucleus in the 575 MeV  $^{36}\text{Ar} + ^{208}\text{Pb}$  reaction can be obtained from published  $B(EL)$  values if the effective nuclear potential is deduced from elastic scattering data measured with high resolution. There is no need to adjust  $B(EL)$  values. The calculations show that at angles forward of grazing the excitation of  $2^+$  states dominates. Even if the relative contribution of unresolved  $3^-$  states were not properly determined due to the lack of additional data we consider the predicted cross sections for GQR excitation as quite reliable. On this basis it is concluded that multiphonon excitations built from giant resonances in the target can hardly be observed at this or even lower beam energies.

## ACKNOWLEDGMENTS

We are thankful to the GSI target laboratory, which provided the  $^{208}\text{Pb}$  target. In particular, we appreciate the help and advice of H. G. Bohlen when performing the coupled-channels calculations. This work has been funded by the German Federal Minister for Research and Technology (BMFT) under Contract No. 06 BO 171.

<sup>1</sup>Jiang Cheng-Lie, P. R. Christensen, O. Hansen, S. Pontopidan, F. Videbaek, D. Schüll, W. Shen, A. J. Baltz, P. D. Bond, H. Freiesleben, F. Busch, and E. R. Flynn, *Phys. Rev. Lett.* **47**, 1039 (1981).

<sup>2</sup>P. Roussel-Chomaz, J. Barrette, B. Berthier, B. Fernandez, J. Gastebois, W. Mittig, Y. Blumenfeld, N. Frascaria, J. P. Garron, J. C. Jacmart, J. C. Roynette, L. Kraus, I. Linck, and Ph. Chomaz, *Phys. Lett. B* **209**, 187 (1988).

<sup>3</sup>M. Beckermann, R. L. Auble, F. E. Bertrand, J. L. Blankenship, B. L. Burks, M. A. G. Fernandes, C. W. Glover, E. E. Gross, D. J. Horen, R. O. Sayer, G. R. Satch-

ler, D. Shapira, Y. Sugiyama, and R. L. Varner, *Phys. Rev. C* **36**, 657 (1987).

<sup>4</sup>P. R. Christensen, S. Pontopidan, F. Videbaek, J. Barrette, P. D. Bond, O. Hansen, and C. E. Thorn, *Phys. Rev. C* **29**, 455 (1984).

<sup>5</sup>F. E. Bertrand, R. O. Sayer, R. L. Auble, M. Beckermann, J. L. Blankenship, B. L. Burks, M. A. G. Fernandes, C. W. Glover, E. E. Gross, D. J. Horen, J. Gomez del Campo, D. Shapira, and H. P. Morsch, *Phys. Rev. C* **35**, 111 (1987).

<sup>6</sup>H. Sohlbach, H. Freiesleben, W. F. W. Schneider, D. Schüll, B. Kohlmeyer, M. Marinescu, and F. Pühlhofer, *Z. Phys.*

- A 328, 205 (1987).
- <sup>7</sup>T. Suomijärvi, D. Beaumel, Y. Blumenfeld, Ph. Chomaz, N. Frascaria, J. P. Garron, J. C. Jacmart, J. C. Roynette, J. Barrette, B. Berthier, B. Fernandez, J. Gastebois, P. Roussel-Chomaz, W. Mittig, L. Kraus, and I. Linck, Nucl. Phys. A491, 314 (1989).
- <sup>8</sup>A. H. Sandorfi, in *Proceedings of the Symposium on Heavy-Ion Physics from 10-200 MeV/u*, edited by J. Barrette and P. D. Bond (Brookhaven National Laboratory, Upton, New York, 1979).
- <sup>9</sup>Ph. Chomaz, N. Frascaria, Y. Blumenfeld, J. P. Garron, J. C. Jacmart, J. C. Roynette, W. Bohne, A. Gamp, W. von Oertzen, M. Buenerd, D. Lebrun, and Ph. Martin, Z. Phys. A 318, 41 (1984).
- <sup>10</sup>Ph. Chomaz, N. Frascaria, Y. Blumenfeld, J. P. Garron, J. C. Jacmart, J. C. Roynette, W. Bohne, A. Gamp, W. von Oertzen, Nguyen Van Gai, and D. Vautherin, Z. Phys. A 319, 167 (1984).
- <sup>11</sup>M. Buenerd, J. Chauvin, G. Duhamel, J. Y. Hostachy, D. Lebrun, P. Martin, P. O. Pellegrin, G. Perrin, and P. de Saintignon, Phys. Lett. 167B, 379 (1986).
- <sup>12</sup>H. G. Bohlen, H. Ossenbrink, H. Lettau, and W. von Oertzen, Z. Phys. A 320, 237 (1985).
- <sup>13</sup>S. Fortier, S. Gales, S. M. Austin, W. Benenson, G. M. Crawley, C. Djalali, J. H. Lee, J. Van der Plicht, and J. S. Winfield, Phys. Rev. C 36, 1830 (1987).
- <sup>14</sup>N. Frascaria, Y. Blumenfeld, Ph. Chomaz, J. P. Garron, J. C. Jacmart, J. C. Roynette, T. Suomijärvi, and W. Mittig, Nucl. Phys. A474, 253 (1987).
- <sup>15</sup>D. Schüll, *The GSI Magnetic Spectrometer*, Vol. 178 of *Lecture Notes in Physics* (Springer, Berlin, 1983), p. 88.
- <sup>16</sup>W. E. Frahn and D. H. E. Gross, Ann. Phys. 101, 520 (1976).
- <sup>17</sup>W. E. Frahn, Nucl. Phys. A272, 413 (1976).
- <sup>18</sup>A. Lell and J. de Boer, Computercode COULEX.
- <sup>19</sup>J. M. Finn, Hall Crannell, P. L. Hallowell, J. T. O'Brien, and S. Penner, Nucl. Phys. A290, 99 (1977).
- <sup>20</sup>P. Ring and J. Speth, Phys. Lett. 44B, 477 (1973).
- <sup>21</sup>J. Raynal, Computercode ECIS79, supplied by Nuclear Energy Agency Data Bank, F91191 Gif sur Yvette, France.
- <sup>22</sup>A. van der Woude, Prog. Part. Nucl. Phys. C18, 217 (1987).
- <sup>23</sup>Ph. Chomaz, N. Van Giai, and D. Vautherin, Nucl. Phys. A476, 125 (1988).
- <sup>24</sup>R. A. Broglia and A. Winther, *Heavy Ion Reactions*, Lecture notes (Benjamin, New York, 1981), Vol. I.
- <sup>25</sup>A. Bohr and B. R. Mottelson, *Nuclear Structure* (Benjamin, New York, 1975), Vol. II.